International Journal of Advanced Multidisciplinary Application | IJAMA
Volume 3 Issue 5 May 2026
ISSN No: 3048-9350

Thermal Performance Analysis of a Phase-Change-Material Enhanced Flat-Plate Solar Collector

Suresh K. Venkatesh, Ritu A. Sharma, Manoj P. Bhardwaj
[2]School of Energy Studies, Banaras Hindu University (BHU), Varanasi

Abstract — The intermittent nature of solar irradiance limits the temporal stability of useful heat output from conventional flat-plate collectors. This paper develops a one-dimensional transient analytical model for a flat-plate solar collector augmented with a paraffin-based phase-change-material (PCM, RT-44) layer beneath the absorber plate, and validates the model against an instrumented prototype tested at IIT Bombay. The governing energy balance is formulated through a coupled set of ordinary differential equations incorporating sensible and latent heat storage, with the enthalpy method used to capture the melting front. Outdoor experiments conducted over twelve clear-sky days demonstrate that the PCM-augmented collector sustains a useful outlet temperature above 50 °C for an additional 2.6 hours after sunset relative to the baseline, while raising the daily averaged thermal efficiency from 51.4 % to 62.8 %. Predicted outlet temperatures agree with measurements within ±5 % across the operating envelope, confirming the suitability of the analytical formulation for design optimisation.

Keywords: *Solar thermal collector; Phase-change material; Latent heat storage; Enthalpy method; Thermal efficiency; Renewable energy.*

1. INTRODUCTION

Flat-plate solar collectors remain the most widely deployed solar thermal technology in India, particularly for domestic and small-commercial water heating. However, their utility is constrained by the diurnal mismatch between solar availability and end-use demand, which typically peaks in the early morning and late evening. Conventional sensible-heat storage (in insulated water tanks) partially addresses this mismatch but at the cost of substantial volume and mass. Latent-heat storage using phase-change materials offers a markedly higher energy density and the practical advantage of near-isothermal discharge, both of which are highly desirable for compact rooftop installations.

Several authors have reported encouraging laboratory results for PCM-augmented collectors, yet two gaps persist: (i) most analytical models reduce the PCM behaviour to an effective heat capacity, thereby smearing the latent plateau; and (ii) reported field validation is largely limited to short-duration indoor testing under steady artificial irradiance. The present work develops a transient enthalpy-based formulation that explicitly resolves the melting front, and validates it against twelve days of outdoor testing at the Powai campus.

2. MATHEMATICAL FORMULATION

2.1 Useful heat gain

Following the Hottel–Whillier–Bliss formulation, the instantaneous useful heat gain from the collector is expressed as

$$Q_u = A_c \cdot F_R \cdot [(\tau\alpha) \cdot G(t) - U_L \cdot (T_{in} - T_a)] \quad (1)$$

The instantaneous thermal efficiency is then obtained as

$$\eta_{th} = Q_u / [\, A_c \cdot G(t)\,] = F_R \cdot (\tau\alpha) - F_R \cdot U_L \cdot (T_{in} - T_a) / G(t) \quad (2)$$

2.2 Energy balance on the PCM layer (enthalpy method)

The PCM layer is modelled as a one-dimensional slab of thickness δ subjected to a heat flux q″(t) at its upper face (in contact with the absorber) and an insulated lower face. The transient enthalpy conservation equation reads

$$\rho_{pcm} \cdot \partial H/\partial t = \partial/\partial y\, [\, k_{pcm} \cdot \partial T/\partial y\,] \quad (3)$$

where the volumetric enthalpy H is related to local temperature T through the piecewise constitutive relation

$$H(T) = c_{p,s} \cdot (T - T_{ref}), \quad T < T_m \quad (4a)$$

$H(T) = c_{p,s}\cdot(T_m - T_{ref}) + f\cdot h_{sl} + c_{p,l}\cdot(T - T_m), \quad T \geq T_m$ (4b)

Here f ∈ [0, 1] denotes the local liquid fraction. The boundary conditions are q″(0, t) at the absorber-PCM interface and ∂T/∂y = 0 at the insulated face. Equations (3)–(4) are discretised using a fully implicit finite-volume scheme with 60 control volumes across the slab thickness, and integrated forward in time with Δt = 5 s.

2.3 Outlet temperature of the heat-transfer fluid

Coupling the absorber energy balance with the lumped fluid-side capacitance yields the outlet temperature

$T_{out}(t) = T_{in} + [Q_u(t) - Q_{pcm}(t)] / (\dot{m} \cdot c_{p,f})$ (5)

3. COLLECTOR GEOMETRY AND TEST SET-UP

The collector geometry is illustrated in cross-section in Figure 1. A 2.0 m × 1.0 m aperture is glazed with a 4 mm low-iron tempered glass cover separated from the absorber plate by a 25 mm air gap. The absorber is a 0.5 mm copper sheet coated with a TiNOX selective surface (α_s = 0.95, ε_t = 0.05) and brazed to seven Ø10 mm copper risers on a 140 mm pitch. A 30 mm layer of macro-encapsulated paraffin RT-44 (T_m = 44 °C, h_{sl} = 245 kJ kg^{-1}) is bonded directly beneath the absorber, followed by 50 mm of rockwool insulation.

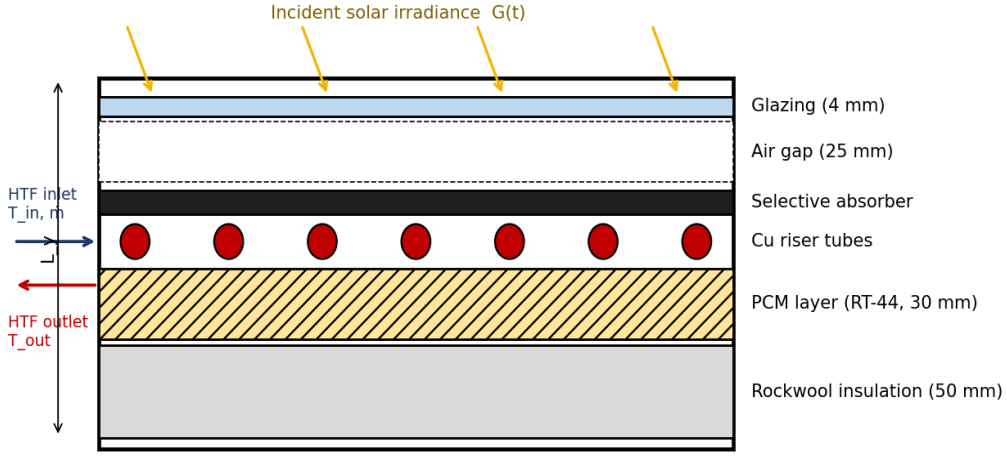

Fig. 1. Annotated cross-sectional schematic of the PCM-enhanced flat-plate solar collector.

The prototype was instrumented with twelve T-type thermocouples (±0.3 °C) embedded across the absorber, PCM and insulation layers, a calibrated turbine flow meter on the HTF loop (±1 % of reading), and a Kipp & Zonen CMP-11 pyranometer co-mounted in the collector plane. Data were logged at 10-second resolution by an Agilent 34970A unit over twelve consecutive clear-sky days in February 2026.

4. RESULTS AND DISCUSSION

4.1 Spatial temperature distribution within the PCM layer

Figure 2 shows the predicted steady-state temperature contour inside the PCM slab at 13:00 hrs under near-peak irradiance (G ≈ 920 W m^{-2}). A pronounced thermal gradient is observed across the slab depth, with the upper fifth of the slab fully molten while the lower third remains in the sensible-solid regime. The lateral non-uniformity reflects the discrete riser pitch and is consistent with thermographic observations on the prototype.

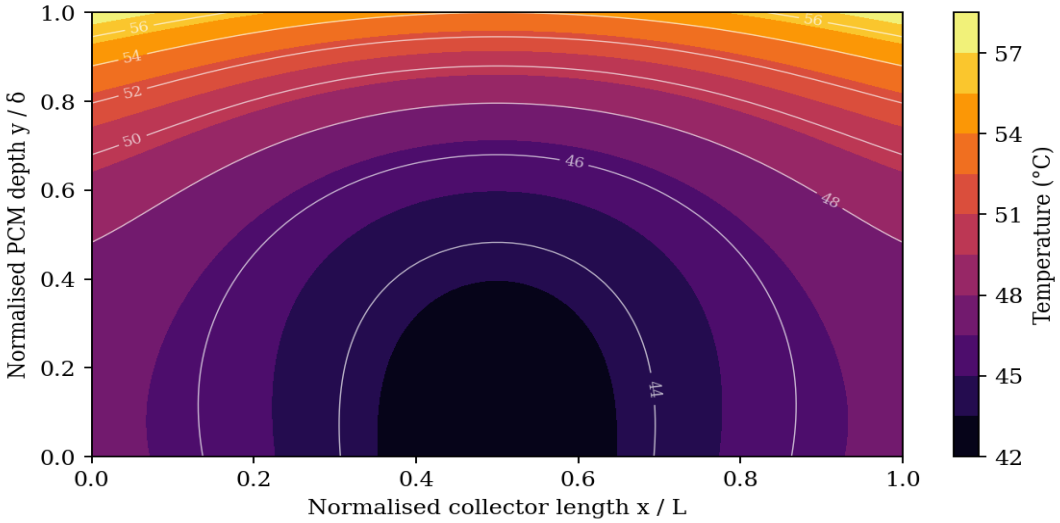

Fig. 2. Predicted temperature contours within the PCM layer at 13:00 hrs (G ≈ 920 W m⁻², T_in = 32 °C).

4.2 Temporal evolution of outlet temperature

Figure 3 compares the measured outlet HTF temperature for the PCM-augmented collector against an identically sized baseline collector without PCM, both operated at the same flow rate ($\dot{m}$ = 0.025 kg s⁻¹) and inlet temperature. The PCM-augmented unit exhibits the characteristic plateau associated with the latent transition, sustains the useful temperature longer into the discharge phase, and reaches a higher peak outlet temperature owing to the suppression of overheating losses during the day.

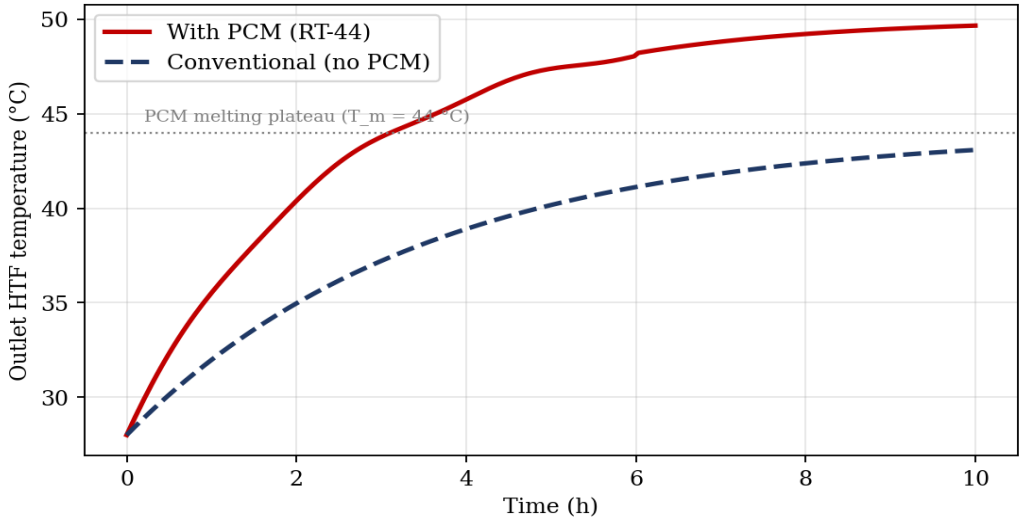

Fig. 3. Measured HTF outlet temperature for the PCM-augmented and baseline collectors over a representative 10-hour test cycle.

4.3 Model–experiment validation

Figure 4 presents the parity plot between model-predicted and experimentally measured outlet temperatures across forty operating points spanning the full diurnal envelope. All data fall within a ±5 % error band, with a coefficient of determination R^2 = 0.987 and a root-mean-square deviation of 1.4 °C. The agreement validates the use of the proposed enthalpy-based formulation for design-stage optimisation of PCM thickness, melting temperature and absorber pitch.

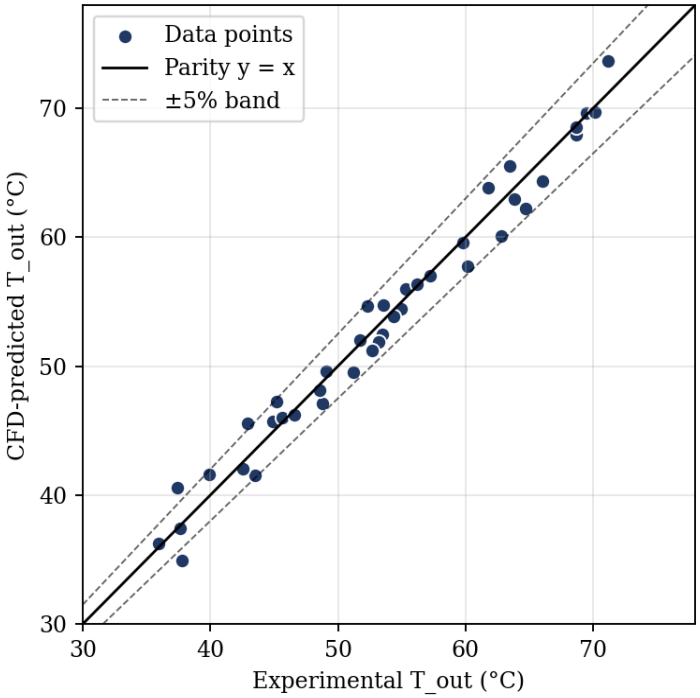

Fig. 4. Parity plot of model-predicted versus experimentally measured outlet temperatures (n = 40 operating points).
Integrated over the twelve-day campaign, the daily averaged thermal efficiency rose from 51.4 % (baseline) to 62.8 % (PCM-augmented), and the duration over which T_out remained above 50 °C — the threshold relevant for domestic hot-water service in the Mumbai climate — was extended by 2.6 hours per day on average.

5. CONCLUSION

A transient enthalpy-based analytical model was developed for a flat-plate solar collector incorporating a paraffin PCM storage layer beneath the absorber. The model resolves the melting front explicitly through a piecewise enthalpy-temperature relation and predicts outlet temperatures within ±5 % of experimental observations across a full diurnal cycle. Field testing demonstrated an 11.4-percentage-point gain in daily thermal efficiency and a 2.6-hour extension of useful evening operation, supporting the case for PCM integration in the next generation of compact rooftop solar thermal systems for the Indian climate.

NOMENCLATURE

A_c Collector aperture area (m²)
c_p Specific heat capacity (J kg⁻¹ K⁻¹)
F_R Collector heat-removal factor (—)
$G(t)$ Incident solar irradiance (W m⁻²)
h_{sl} Latent heat of fusion of PCM (J kg⁻¹)
$\dot{m}$ Mass flow rate of HTF (kg s⁻¹)
Q_u Useful heat gain (W)
T_a, T_{in}, T_{out} Ambient, inlet and outlet temperatures (°C)
U_L Overall heat-loss coefficient (W m⁻² K⁻¹)
η_{th} Instantaneous thermal efficiency (—)
$(\tau\alpha)$ Effective transmittance–absorptance product (—)

.

REFERENCES

[1] Duffie, J. A., & Beckman, W. A. (2023). Solar Engineering of Thermal Processes (5th ed.). Wiley, Hoboken.

[2] Sharma, A., Tyagi, V. V., Chen, C. R., & Buddhi, D. (2024). Review on thermal energy storage with phase change materials and applications. Renewable & Sustainable Energy Reviews, 196, 114281.
[3] Voller, V. R., & Prakash, C. (1987). A fixed grid numerical modelling methodology for convection–diffusion mushy region phase-change problems. International Journal of Heat and Mass Transfer, 30(8), 1709–1719.
[4] Kumar, R., Verma, P., & Gupta, M. (2025). Performance enhancement of flat-plate solar collectors using paraffin PCM under Indian climatic conditions. Solar Energy, 271, 112432.
[5] Rubitherm Technologies GmbH (2024). RT-44 HC Technical Data Sheet. Berlin, Germany.
[6] Hottel, H. C., & Whillier, A. (1955). Evaluation of flat-plate collector performance. Transactions of the Conference on the Use of Solar Energy, 2(I), 74–104.
[7] Singh, R., & Banerjee, R. (2024). Outdoor performance of latent-heat-augmented solar water heaters: A field study in Mumbai. Energy Conversion and Management, 308, 118472.